applied sciences

MDPI

Article

Green Hydrogen Storage in an Underground Cavern: A Case Study in Salt Diapir of Spain

Laura M. Valle-Falcones [1,*], Carlos Grima-Olmedo [1], Luis F. Mazadiego-Martínez [2], Antonio Hurtado-Bezos [3], Sonsoles Eguilior-Díaz [3] and Ramón Rodríguez-Pons [1]

[1] Departamento de Ingeniería Geológica y Minera, Escuela Técnica Superior de Ingenieros de Minas y Energía, Universidad Politécnica de Madrid, Ríos Rosas 23, 28003 Madrid, Spain; carlos.grima@upm.es (C.G.-O.); ramon.rodripons@upm.es (R.R.-P.)
[2] Departamento de Energía y Combustibles, Escuela Técnica Superior de Ingenieros de Minas y Energía, Universidad Politécnica de Madrid, Ríos Rosas 23, 28003 Madrid, Spain; luisfelipe.mazadiego@upm.es
[3] Centro de Investigaciones Energéticas, Medioambientales y Tecnológicas, Avda. Complutense 40, Edif. 20, 28040 Madrid, Spain; antonio.hurtado@ciemat.es (A.H.-B.); sonsoles.eguilior@ciemat.es (S.E.-D.)
* Correspondence: lauramaria.valle@upm.es; Tel.: +34-910676499

Featured Application: The underground salt cavern design by leaching process for green hydrogen storage to compensate for the variable/seasonal nature of renewables and increase the availability of a clean fuel to society.

Abstract: The Poza de la Sal diapir is a closed circular depression with Cretaceous Mesozoic materials, formed by gypsum, Keuper clays, and a large extension of salt in the center with intercalations of ophite. The low seismic activity of the area, the reduced permeability and porosity of the salt caverns, and the proximity to the Páramo de Poza wind park, make it a suitable place for the construction of a facility for underground storage of green hydrogen obtained from surplus wind power. The design of a cavern for hydrogen storage at a depth of 1000 m takes into account the differences in stresses, temperatures, and confining pressures involved in the salt deformation process. During the 8 months of the injection phase, 23.0 GWh can be stored in the form of hydrogen obtained from the wind energy surplus, to be used later in the extraction phase. The injection and extraction ratio must be developed under the conditions of geomechanical safety of the cavity, so as to minimize the risks to the environment and people, by conditioning the gas pressure inside the cavity to remain within a given range.

Keywords: green hydrogen; energy vector; water electrolysis; wind power; geological storage; leaching process

Citation: Valle-Falcones, L.M.; Grima-Olmedo, C.; Mazadiego-Martínez, L.F.; Hurtado-Bezos, A.; Eguilior-Díaz, S.; Rodríguez-Pons, R. Green Hydrogen Storage in an Underground Cavern: A Case Study in Salt Diapir of Spain. *Appl. Sci.* **2022**, *12*, 6081. https://doi.org/10.3390/app12126081

Academic Editors: Jorge Loredo and Javier Menéndez

Received: 17 May 2022
Accepted: 13 June 2022
Published: 15 June 2022

1. Introduction

Due to concerns about climate change and the harmful effects on the environment caused by the use of fossil fuels as the main source of energy, in addition to those caused by the security of energy supplies, many analysts have considered hydrogen as a potential alternative energy source.

To meet the sustainable development goals, the International Energy Agency (SDS) has highlighted the fundamental role of hydrogen within the new energy model. The United Nations Industrial Development Organization [1] has defined hydrogen as the paradigm shift for efficient energy storage. The Ministerio para la Transición Ecológica y el Reto Demográfico of Spain [2] considers that this element is essential to the decarbonization of some sectors, such as transportation, electricity, and heat generation.

The main characteristic of hydrogen is its function as an "energy vector", since, although it needs an energy input to be generated, it is capable of storing and releasing this energy when required. Hydrogen is a colorless, odorless, tasteless, and non-toxic gas, found

in air at concentrations of 100 ppm [3]. At the Earth's surface, it is found as a compound together with other elements, such as oxygen, carbon, or nitrogen [4]. It has a higher energy density per unit mass than the other hydrocarbons, with a LHV and specific gravity, respectively, of 120 MJ/kg (×3 gasoline) and 0.089 (÷10 natural gas) in NC, in addition to a reduced level of pollutant emissions. However, it requires a larger storage volume to generate the same energy as other fuels (×4 gasoline) [5,6], which makes large-scale storage and long-distance transport more expensive. Depending on the raw material used to generate hydrogen and the CO_2 emissions associated with its production, it is classified in decreasing order of environmental impact as gray, blue, or green. Hydrogen consumption in Spain is around 500,000 ton/year and it is used as a raw material in refineries (70%), in the chemical industry (25%), and in other sectors such as metallurgy [7]. This hydrogen is 99% gray hydrogen, obtained from the particular production processes of each industry, and can be replaced by green or renewable hydrogen.

Renewable energies in Spain have a large share in the energy mix, accounting for 54.0% in 2020 (Figure 1). Wind power, which represents almost 50% of the generated renewable energy, is the technology with the highest share (24.8%) in the power structure, producing 27.5 GW.

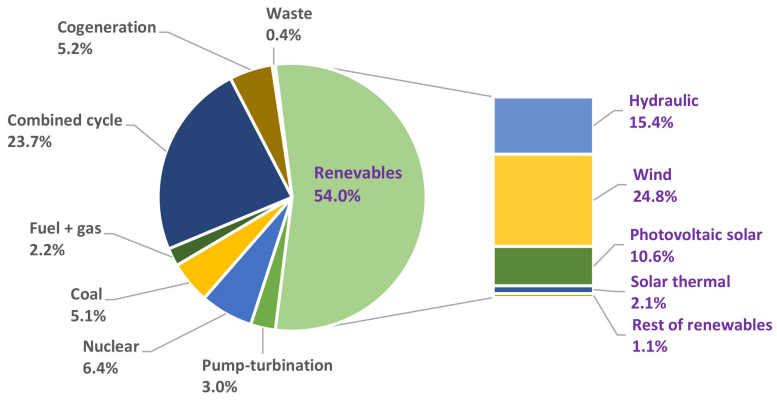

Figure 1. Renewable energies in the Spanish electrical system 2020 [6].

Spain is the second-ranked country in Europe in terms of the installed wind power capacity, well behind Germany, which has just over 60 GW, with France in third place with about 18 GW. In terms of the contribution of this source to total electricity generation, the leader is be Denmark, with nearly 60% of its production coming from wind, and Spain is in seventh place [8]. Furthermore, the great variability of wind power means that the contribution of wind power generation to the hourly coverage of electricity demand varies considerably.

Globally, in 2020, onshore wind power capacity was installed in Asia-Pacific (336,286 MW), Europe (194,075 MW), Americas (169,758 MW), and Africa, Middle East (7277 MW); and offshore in Europe (24,837 MW), Asia-Pacific (10,414 MW), Americas (42 MW), and Africa, Middle East (0 MW). Figure 2 shows the total values of installed wind power capacity for onshore (707.4 GW) and offshore (35.3 GW), and the percentage contribution by country.

Hydrogen is generated inside alkaline and proton exchange membrane electrolyzers. The passage of electricity between two electrodes (anode and cathode) immersed in water produces its dissociation through a process of electrolysis. The use of solar or wind energy allows a "power to gas" hydrogen generation process [9]. Its seasonal storage in pipelines, vessels, or underground formations (depleted gas fields, aquifers, salt caverns, etc.), enables the subsequent use of fuel cells to produce green electricity during periods of low "power to power" generation [10]. Another important ecofriendly use would be its blending with natural gas and its transportation by pipeline or its joint storage with natural gas. Compared with methane, hydrogen has lower solubility. This is considered to be an advantage because, in a hydrogen–methane–brine system, a smaller hydrogen loss due to dissolution is expected.

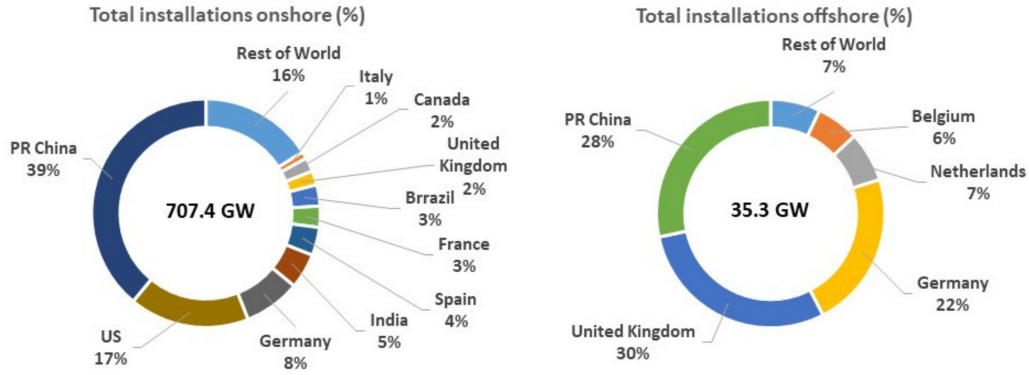

Figure 2. Total installed wind power onshore/offshore 2020. Global Wind Energy Council (GWEC).

The supply of hydrogen to the local industry and mobility sectors, in addition to an increased connection to the main gas and electricity infrastructure, means that the need for large-scale underground storage of renewable hydrogen is expected to increase significantly.

Underground geological reservoirs allow the safe storage of large volumes of hydrogen, at high pressures with high energy densities, without the environmental impact caused by surface tanks [8,11]. Salt caverns offer one of the most promising options due to their low investment cost, low permeability and porosity, and their inert nature, which prevents contamination of the stored gas [12].

In water–hydrogen–salt systems of a storage type, the presence of salt decreases the solubility of hydrogen in the brine, preventing gas loss by dissolution in water. However, there may be operating conditions that could cause disturbances such as dilatation and damage of the salt rock, with an increase in permeability and a decrease in strength [7,13].

Due to its climatic conditions of wind generation and the presence of a large number of underground salt structures, Spain is a country with great potential as a producer and storer of hydrogen. This work establishes the geological and design requirements for injection and underground storage in salt cavern to ensure the permanence of the gas and safety for people and the environment.

2. Poza de la Sal

For the geological storage of any gas, geological, economic, technical, and safety factors must be taken into account, both for the population and the environment [12,14], in order to guarantee the required capacity, confinement, and integrity. In general, sedimentary basins present favorable conditions for gas storage because, unlike cratons and orogens, they do not have excessive fracturing.

The site chosen for the underground hydrogen storage is the salt diapir of Poza de la Sal, located in the north of the province of Burgos (Castilla y León). It is an area of very low seismic activity, reducing the risk of fractures opening up to allow gas migration to the outside.

The Poza de la Sal diapir is adjacent to the Páramo de Poza WP (Figure 3), which has 133 wind turbines and a total installed capacity of 99.75 MW. This facility would generate green hydrogen from surplus wind energy at times when power generation exceeds demand, to be stored for later use.

A circular depression can be seen in the landscape due to the dissolution and erosion of the superficial envelope of the salt, composed of gypsum and clay, with the volcanic rocks of ophitic texture that were trapped between the soft materials highlighted in the center.

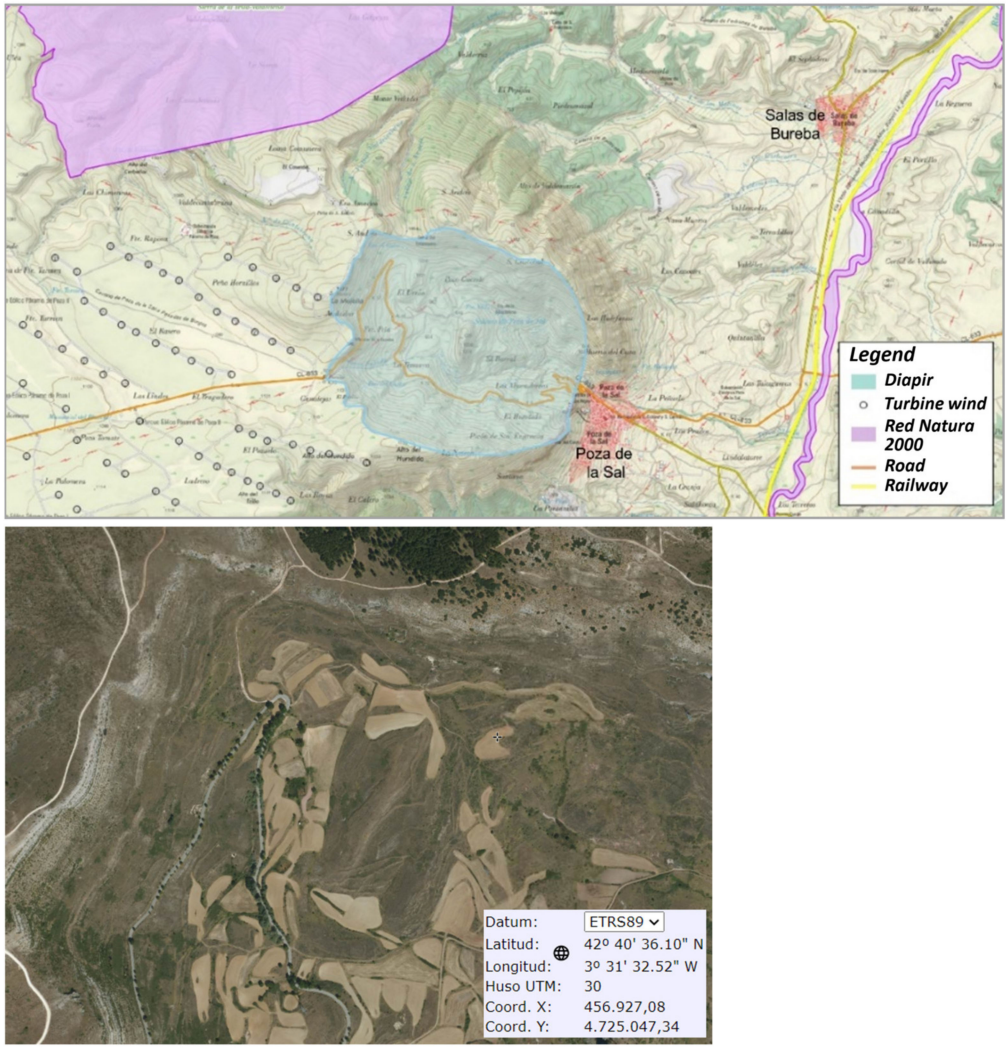

Figure 3. Location and environment of the diapir of Poza de la Sal.

2.1. Regional Geology

The Basque-Cantabrian Basin is in the eastern part of the Cantabrian Range and includes western Navarre, the Basque Country, northern Burgos and Palencia provinces, and part of Cantabria. The western part of the Basque-Cantabrian Basin is separated from the Basque Paleozoic Massifs and the Pyrenees by the Pamplona fault, whereas it is limited to the west by the Asturian Paleozoic Massif. It is comprised of the Bay of Biscay to the north and to the south, and of the thrust over the Tertiary Duero and Ebro Basins.

The basin underwent a complex and prolonged evolution as it adapted to the dominant tectonic processes. In the Upper Permian, a submerged sea began to form as the continental crust underwent a hyperextensional process, stretching and sinking due to different tectonic and thermal processes until its thickness was reduced to one-third of its original thickness. This environment favored the deposition of sediments for 250 million years, the most important being the Mesozoic materials, which reached thicknesses of between 12 and 17 km (8 and 17 miles) [15]. Submarine volcanic processes also took place, but without the formation of an oceanic crust. This extensive stage was replaced by compressive forces in the Miocene, when the African plate began to move towards Eurasia, and the collision between them caused the emersion of the entire accumulated stratigraphic series (Figure 4).

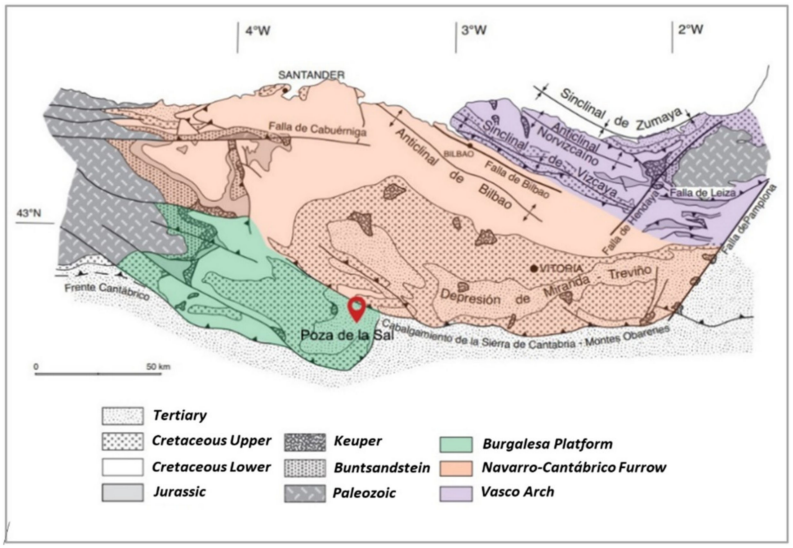

Figure 4. Geology of the Basque-Cantabrian Basin [16].

2.2. Geological Structure

In the Upper Triassic, also known as Keuper, what we know today as the Basque-Cantabrian Basin was a shallow sea that was beginning to form due to extensive movements of the Earth's crust. This transitional environment between continental and marine, known as the Sabkha environment, was characterized by an extremely arid climate, which evaporated large masses of salt water, favoring the precipitation of carbonates, sulfates, and chlorides. At the same time, the rivers deposited fine sediments: clays, silts, and sands. Volcanic materials were also expelled and trapped in the sediments as they cooled. These materials that make up the Keuper Facies reached a thickness of 400–500 m.

Marine sedimentation continued during the Jurassic and Cretaceous, so that the strata reached considerable thickness when halokinetic salt movements began. As marine regression took place and emerged zones arose, the salts continued to ascend until they broke through the rock cover (Figure 5).

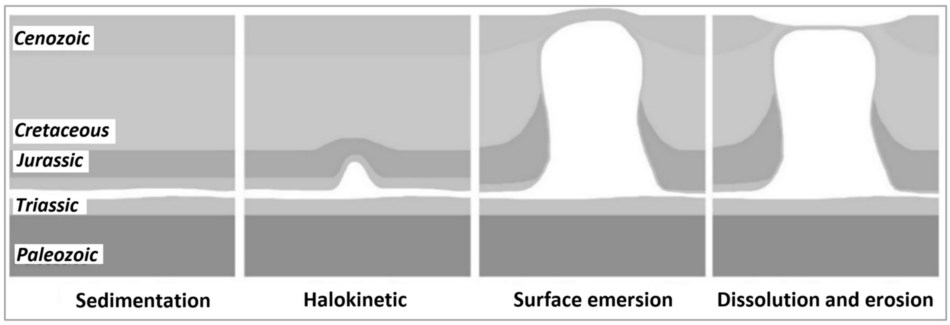

Figure 5. Salt diapir formation process.

2.3. Geomorphology

The formation is recognizable in the landscape because a circular depression has formed due to the dissolution and erosion of the superficial salt envelope, composed of gypsum and clays, with volcanic rocks of ophitic texture standing out in the center, trapped between the soft materials. The water infiltrating through the surface cracks is capable of dissolving chlorides (halite), but not sulfates (anhydrite) or clays. However, when anhydrite is hydrated, it becomes gypsum, which has very high solubility.

The depth reached by the salt is not known exactly but, due to the great thickness of the materials that covered it, it may be several kilometers. The caverns in geological structures associated with the salt deposits usually occur at depths of 300–2000 m [17].

3. Methodology and Results

3.1. Storage Design

The design of the cavities must ensure their stability, tightness to the stored gas, acceptable surface subsidence, and the environmental safety of the surroundings. These requirements have to be met both during the leaching process for cavern excavation and during gas injection and extraction operations. The permeability of the salt rock is mainly affected by the stress conditions and the operating pressure requirements of the storage gas [7]. In addition, from an economic point of view, the optimization of its shape and size is sought in order to store the largest amount of gas. The storage capacity is calculated on the basis of thermodynamic considerations according to the specific data of the storage facility [12].

Salt caverns intended for storage must be carefully designed according to the specific properties of the salt and the precise operating circumstances.

The estimated cavern construction time of 1–3 years [18] and up to 5 years [11] varies according to the dimensions to be achieved, the structure and composition of the salt rock, and the leaching method employed [19]. To carry out the leaching process, the drilling of a well is required, which, after a specific and adequate completion, will constitute the H_2 injection well in the cavern.

3.1.1. Drilling of the Well-Cavern Construction

In order to devise a drilling design that ensures the stability of the well in the short and long term, the following is a description of the aspects that must be taken into account when drilling through salt masses, in addition to the problems that may occur and the best way to solve them.

Salt creep behavior can cause problems in the drilling stages of the well if not properly designed. For this, all aspects involved in the salt deformation process must be taken into account: stress difference, temperature, confining pressure, grain size, and the presence of water inclusions or gas bubbles [20]. The first two are the most influential on salt creep and, therefore, on wellbore stability.

When drilling begins and the natural stress state is altered, salt flows to restore equilibrium at a rate proportional to the stress difference (between that exerted by the formation and the hydrostatic pressure of the drilling mud) and to the temperature, which increases with depth. The main recommendations to avoid this behavior are as follows:

- The drilling mud must exert a hydrostatic pressure equal to the horizontal stress. Although the earth stress increases with depth, the hydrostatic pressure of the mud will increase accordingly, counteracting the stresses. Water- or oil-based muds are used to pass through salt formations [20]. Since the latter are more expensive and polluting, an aqueous mud saturated in salt will be used in order to avoid dissolution of the borehole walls.
- The casing design must be based on the stresses that the rock will exert, and the chosen material must have sufficient strength to prevent deformation and collapse. Long-term stability must be considered as halite remains relatively stable during drilling but continues to deform over decades of the well's life [21].
- To isolate the wellbore and prevent the application of non-uniform loads on the casing, the annular spaces between the casings should be filled with cement having high salt concentrations to prevent dissolution of the formation and additives to aid mixing and setting [20].

3.1.2. Cavity Shape

The shape of the cavity affects the spatial distribution of stresses and, thus, the convergence of the salt rock and the volume loss of the cavern. Proper design of its shape will increase stability and safety, so models should be made once the geomechanical parameters obtained from laboratory samples are known, although the actual shape of the cavern will be more complex than the simulated one.

The caverns can have cylindrical, elliptical, or truncated cone shapes, extending the roof or the bottom of the cavity. The best performance (higher stability, lower stress state, and lower convergence) is obtained for cylindrical caverns with rounded edges [12,22], i.e., with hemispherical shapes at the top and bottom of the cylinder, giving rise to a capsule shape.

3.1.3. Cavity Size

In salt domes, due to their great thickness, unlike in stratified salt deposits, there are no space restrictions. The dimensions of the cavity are usually established by maintaining a height/diameter ratio equal to 5 [12,23], i.e., in this case, for a diameter of 48 m, a height of 240 m.

The volume of the capsular shape is determined with Equation (1).

$$V = \pi \times R^2 \times (H - D) + \frac{4}{3} \times \pi \times R^3 \quad (1)$$

The volume obtained for the cavity, 515,355 m^3, is within the usual values considered by other authors of 500,000 m^3–750,000 m^3 [11,12].

3.1.4. Leaching Brine Management

Approximately 7 m^3 of water will be required to dissolve 1 m^3 of salt [24], about six times more than that corresponding to each open cavern, which represents a demand during the leaching process of at least 3 million m^3 of fresh water per cavern. As the Torca Salada stream and the Homino river are located near the project site, it is feasible to use their waters by requesting the corresponding water use permit from the Ebro Hydrographic Confederation.

The volume of brine obtained will be greater than the volume of fresh water, since it comes out loaded with salt. Adding the volume of water that we introduce and the volume of each leached cavern, we obtain a brine volume of approximately 3.5 million m^3 (Equation (2)).

$$V_{brine} = V_{water} + V_{rock} \quad (2)$$

In order to assess the destination of the brine as a commercial by-product, the quantity obtained must be calculated (Equation (3)).

$$m_{brine} = \rho_{water} \times V_{water} + \rho_{rock} \times V_{rock} \quad (3)$$

The densities of fresh water, salt rock, and produced brine are 1, 2.16, and 1.17 g/cm^3 respectively, resulting in a brine mass of 4.2 million tons.

The brine is to be discharged into a specially constructed surface raft for subsequent sale to the chemical industry.

3.2. Operational Parameters

3.2.1. Temperature in the Cavern

The temperature of the hydrogen inside the cavern is assumed to be equal to that of the surrounding rock.

Once the surface temperature and the temperature–depth gradient are known, the temperature of the cavity can be calculated as being lower at the top than at the bottom. For the calculations, the average temperature between these points is considered (Equation (4)).

$$T_a = T_{sup} + \nabla T \times (z - (H/2)) \quad (4)$$

The base of the cavity is located at a depth of 1000 m, so taking a surface temperature of 10.5 °C (annual average in the province of Burgos) and a temperature gradient of 25 K/km, we obtain an average temperature of 32.3 °C in the cavity.

In the same way, the temperatures at the ceiling (29.0 °C) and at the bottom (35.5 °C) of the cavern are obtained, resulting in a temperature increase of 6.5 K.

3.2.2. Lithostatic or Overpressure

Prior to opening the cavern, there are natural stresses in the ground that are assumed to be isotropic [14,20], i.e., the horizontal pressure is equal to the vertical pressure.

The average density of the rock is 2.30 g/cm^3 because most of the overburden is salt (density of 2.16 g/cm^3), with a few meters near the surface consisting of gypsum, shale, and anhydrite. In addition, since this is a rock with such low permeability and porosity, hydrostatic pressure is not considered.

As with the temperature, the pressure at the top of the cavern will be lower than that at its base. For the calculations, the lithostatic pressure at the center of the cavern is considered (Equation (5)).

$$P = \rho \times g \times (z - (H/2)) \quad (5)$$

This results in a lithostatic pressure of 19.6×10^6 Pa, equivalent to 19.6 MPa (196 bar).

3.2.3. Operating Pressure

The opening of the cavern implies a modification of the natural tensional state, inducing tensions that must be regulated with the pressure of the stored gas. To achieve the geomechanical safety of the cavern, the pressure of the gas inside the cavern must remain between maximum and minimum pressure values. If the pressure rises above the maximum pressure, fractures may appear in the rock with gas migration channels. If the pressure drops below the minimum pressure, dilatation phenomena occur with the opening of microfractures that increase the volume and permeability of the rock, decreasing the volume of the cavity and endangering its stability.

The establishment of working pressure limits is based on conventional criteria and geomechanical studies of the site. Values of 85% and 80% of the lithostatic pressure are proposed for the maximum pressure, whereas the values of 30% and 24% of the overburden pressure are proposed for the minimum pressure [7,11,12].

Adopting the most conservative criterion, the maximum and minimum operating pressures will be, respectively (Equations (6) and (7)):

$$P_{max} = 0.8 \times P \quad (6)$$

$$P_{min} = 0.3 \times P \quad (7)$$

For the pressure calculated above, a maximum value of 15.84 MPa (158 bar) and a minimum of 5.94 MPa (59 bar) is obtained. These pressures are within the usual operating ranges 100–270 bar for the maximum and 35–90 bar for the minimum [11,23,25].

3.2.4. Density of Hydrogen Storage

Hydrogen at high pressures no longer behaves as an ideal gas, and a compressibility factor must be used in the equation of state. This factor depends on temperature and pressure (real gas equation of state). The maximum and minimum densities are obtained [26] for the average temperature calculated in the cavern and the maximum and minimum pressures that the gas will have according to its tensional state (Equations (8) and (9)).

$$\rho_{H_2,\,max} = \frac{P_{max} \times M}{Z_1 \times R_0 \times T} \quad (8)$$

$$\rho_{H_2,\,min} = \frac{P_{min} \times M}{Z_2 \times R_0 \times T} \quad (9)$$

The molecular mass of hydrogen is 2.016 g/mol and the gas constant is 8.314 J/K·mol. The compressibility factors are calculated with Table 1 or through a program [27], thereby

obtaining values of Z1 and Z2 of 1.09447 and 1.03525, respectively, from the temperature and the maximum and minimum pressure.

Table 1. Hydrogen compressibility factors.

		Temperature (K)						
		250	**273.15**	**298.15**	**350**	**400**	**450**	**500**
Pressure (bar)	1	1.00070	1.00004	1.0006	1.00055	1.00047	1.00041	1.00041
	5	1.00337	1.00319	1.00304	1.00270	1.00241	1.00219	1.00196
	10	1.00672	1.00643	1.00605	1.00540	1.00484	1.00435	1.00395
	50	1.03387	1.03235	1.03037	1.02701	1.02411	1.02159	1.01957
	100	1.06879	1.06520	1.06127	1.05369	1.04807	1.04314	1.03921
	150	1.10404	1.09795	1.09189	1.08070	1.07200	1.06523	1.05936
	200	1.14056	1.13177	1.12320	1.10814	1.09631	1.08625	1.07849
	250	1.17789	1.16617	1.15499	1.13543	1.12034	1.10793	1.08764
	300	1.21592	1.20101	1.18716	1.16300	1.14456	1.12957	1.11699
	350	1.25461	1.23652	1.21936	1.19051	1.16877	1.15112	1.13648
	400	1.29379	1.27220	1.25205	1.21842	1.19317	1.17267	1.15588
	450	1.33332	1.30820	1.28487	1.24634	1.21739	1.19439	1.17533
	500	1.37284	1.34392	1.31784	1.27398	1.24173	1.21583	1.19463
	600	1.45188	1.41618	1.38797	1.33010	1.29040	1.2592	1.23373
	700	1.53161	1.48880	1.44991	1.38593	1.33914	1.30236	1.27226

The value obtained for the maximum density is 11.4 kg/m^3 and that for the minimum density is 4.51 kg/m^3.

3.2.5. Mass of Gas

A part of the hydrogen stored (base gas or cushion gas) must always remain in the cavity in order to maintain the minimum operating pressure that ensures its stability. The rest of the stored hydrogen (working gas) can be withdrawn when required for consumption. From the base mass and total mass of stored gas, the working mass of the cavern can be calculated (Equation (10)).

$$m_{work} = m_t - m_{base} = V \times (\rho_{max} - \rho_{min}) \quad (10)$$

The result obtained is 3.5 and 2.3 million kilograms of working gas and base gas, respectively, totaling 5.8 million kilograms of stored hydrogen. The obtained amount of base gas with respect to the total is 39.6%, a value that is within the range considered by other authors, i.e., 1/3–2/5 [7,11,28].

3.3. Energy Balance

Figure 6 shows the scheme of hydrogen generation with renewable wind energy, and the process of storage (injection) and production (extraction) from inside the cavern in the salt diapir.

The energy balance associated with the loading and unloading of hydrogen in the storage facility was calculated taking into account the energy consumption of Castilla y León in 2020, assuming that it is constant throughout the year. Wind energy production [6] in that year was 12,576 GWh, compared to 22,147 GWh of total renewable energy production.

In the Autonomous Community of Castilla y León during the months of October to June, wind energy production is higher than its consumption, due to more favorable wind conditions in autumn and winter. Conversely, an extra supply of energy is needed in the period from July to September [6].

The energy study considers, in the first period, the accumulation of excess wind energy in the form of hydrogen injected into the salt cavern, in order to allow this energy to be recovered in the extraction phase.

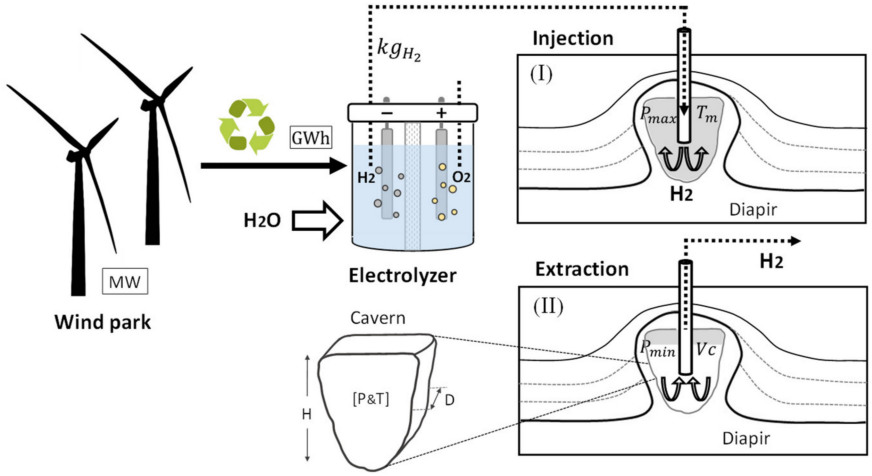

Figure 6. Typical scheme of the process of generation, injection, and extraction of green hydrogen.

An electrolyzer needs about 48 kWh to produce 1 kg of hydrogen [7] with an efficiency of 70%. The electrolysis process to be able to fill a cavern resulting in a quantity of energy consumed is calculated in Equation (11).

$$\mathrm{ECE} = 48 \times 10^{-6} \frac{\mathrm{GWh}}{\mathrm{kg_{H_2}}} \times 5.8 \times 10^{6} \mathrm{kg_{H_2}} = 279\ \mathrm{GWh} \tag{11}$$

Considering a hydrogen storage efficiency in salt caverns of 98% (IEA, 2019), 396 GWh would need to be provided for the total amount of gas in the first year of storage.

The energy content of the working gas can be calculated (Equation (12)):

$$\mathrm{C} = \mathrm{m_{work}} \times \mathrm{LHV} \tag{12}$$

The LHV of hydrogen, 33.3 kWh/kg, represents the energy released as heat due to its combustion, resulting in a cavern capacity of 117×10^6 kWh or 117 GWh.

Following the average wind energy cycle in Castilla y León, an excess of 4% of this energy was estimated between October and June [29].

The wind turbines of the WP Páramo de Poza have a total power of 99.75 MW, which allows the calculation of the surplus energy produced during an 8-month period (Equation (13)).

$$\mathrm{WES} = 99.75\ \mathrm{MW} \times 8\ \mathrm{meses} \times 30\ \mathrm{day/mes} \times 24\ \mathrm{h/day} \times 0.04 = 23.0\ \mathrm{GWh} \tag{13}$$

As the excess wind energy produced by the WP Páramo de Poza is less than the capacity of the cavern, it is possible to receive and store renewable energy from other wind farms in the form of hydrogen.

Given the dimensions of the diapir of Poza de la Sal and the fact that, in Castilla y León, 57% of the renewable energy generated is of wind origin, the possibility of building two caverns with the same dimensions is being considered. They will allow for simultaneous injection in one of them and hydrogen production in the other, thus providing a total capacity of 396 × 2 = 792 GWh; that is, the energy necessary for providing the total amount of gas in the first year of storage. Consequently, 4% of the surplus of the 12,576 GWh of wind energy generated in all of Castilla y León in 2020 (503 GWh) could be stored in the two caverns. The distance between the longitudinal axes of both caverns must be four times greater than their diameter [12], i.e., 192 m, to ensure the stability of the storage.

3.4. Operation

The well must be completed before the cavities begin to function as hydrogen stores. The production tubing should be placed and the remaining brine removed, then the wells prepared for safe gas injection and production.

The first hydrogen filling is carried out when the leaching is finished and the caverns have design dimensions that will favor the removal of the residual brine. For this purpose, the production pipe is placed, which replaces the larger diameter leaching pipe, while the smaller diameter pipe remains in the well for brine extraction.

Injection and Extraction of Hydrogen

The ratio of injection and extraction of hydrogen from the cavity is limited by the maximum and minimum pressure, by the maximum pressure change per unit time that allows its stability, and by the maximum flow velocity inside the production tubing, which depends on its diameter [11,26].

The maximum pressure is reached at the end of hydrogen injection and the minimum pressure occurs when the working hydrogen is extracted, with a portion remaining as a cushion gas to ensure stability. In addition to this function, the base gas provides the pressure necessary to produce the working hydrogen.

The mass of hydrogen injected will depend on its density, which is a function of the operating pressure and temperature. The injection ratio is conditioned by the pressure ranges to be maintained in the salt cavern, and in no case should the maximum pressure of 158 bar be exceeded. Assuming a constant injection rate during the months of October to June of 0.34 kg/s (30 ton/day) [29], obtained by simulation studies, the amount of hydrogen stored in the cavern can be calculated (Equation (14)).

In the unloading of the storage during the months of July to September, a lower extraction rate of 0.24 kg/s (21 ton/day) is considered, due to the decrease in the pressure in the cavern, and consequently, to the decrease in the hydrogen density (Equation (15)).

$$H_2\text{injected} = 30\frac{\text{ton}}{\text{day}} \times 30\frac{\text{day}}{\text{month}} \times 8\ \text{month} = 7200\ \text{ton} \quad (14)$$

$$H_2\text{produced} = 21\frac{\text{ton}}{\text{day}} \times 30\frac{\text{day}}{\text{month}} \times 4\ \text{month} = 2520\ \text{ton} \quad (15)$$

The percentage of hydrogen recovered, that is, the ratio of hydrogen produced to hydrogen injected, is 35%, providing 84 GWh of energy.

4. Discussion

Spain has a land area of 50 million hectares and large territories with low population density, and experiences Mediterranean and Atlantic winds; hence, it is among the European countries having the greatest potential for the use of renewable energies. Major technological improvements in recent years have led to the implementation of numerous renewable energy production facilities, especially in the form of photovoltaic cells and wind turbines.

Due to the variation in solar radiation and the volatile nature of wind, renewable energy production fluctuates, preventing the supply of a reliable baseload. Renewable energy storage would allow short-term and seasonal imbalances to be compensated for, and the excess production during low demand hours to be used.

Hydrogen is a fuel that has a high energy density per unit mass, but very low energy density per unit volume, in both liquid and gaseous states. The availability of an adequate storage system is one of the major obstacles to its large-scale use. It requires large volumes associated with high pressures (700 bar), low liquefaction temperatures (−253 °C), or its combination with other heavier materials [30].

Hydrogen may be transported through natural gas pipelines and infrastructure, in variable proportions of up to 10–20%, limited by specific regulations of each country, supply pressure, and end use (domestic, industrial, energy, etc.) [31,32]. This aspect enables the coupling of the gas and electricity sectors, thereby allowing for joint demand management.

Furthermore, an improvement and optimization of the energy system would result in flexibility of the electricity system, which is essential to achieve a high penetration of non-manageable renewable generation.

The development of the chemical process by electrolysis and its underground storage in appropriate geological structures for subsequent consumption in fuel cells, or injection into the local distribution or transport network, is of particular relevance in the implementation of hydrogen technology.

The high diffusivity of hydrogen makes it capable of diffusing even through solids, resulting in a loss of the stored fuel and its release into the atmosphere. Another aspect to consider, especially at high pressure, is the possible embrittlement of the metals or geological formations used for its confinement, in addition to the increase in its permeability. In this sense, salt caverns are suitable underground storages for pure H_2(g), providing a good seal and a very low permeability, which ensures a minimum loss of hydrogen and a very low risk of contamination with impurities from the environment.

The structural and design characteristics of the salt cavern will determine the amount of hydrogen that can be stored within the formation. Safety standards and risk analysis tools similar, for example, to those developed by the refining industry should be adopted during use. This will enable the application of best practices in new green hydrogen plants, and the use of optimized maintenance, reliability, and incident response strategies.

The study of H_2 storage in porous media such as aquifers generally has the advantage of higher capacity and availability in the subsurface. Although they have similar geological characteristics to depleted hydrocarbon reservoirs, which were originally gas filled, they require more precise geological studies and analyses of porosity and permeability, in combination with the presence of a suitable seal formation to ensure the tightness of storage.

Leaching cycles are well developed in evaporite rocks such as rock salt (halite) and potash, which dissolve at a high rate [11]. The irregular shape of the caverns is a consequence of the presence in the salt formations of water-insoluble interlayers, such as anhydrites and shales, reducing their volume and utilization rate [10].

The brine extracted from the cavity can have three final destinations:

- Discharge to the sea;
- Geological injection and reuse; and
- Treatment or sale of salt

Due to the great distance to the sea, the difficulty in finding a geological structure capable of storing the brine, and the high costs of its treatment in the project itself, the option of discharging it in a raft, built for this purpose, on the surface for subsequent sale to the chemical industry is proposed.

The smaller extent and more defined geometry of salt caverns means that they require less cushion gas than depleted hydrocarbon reservoirs and aquifers having wide, elongated structures. The cushion gas requirement in an aquifer could be as much as 80% of the total reservoir capacity compared to 50–60% in depleted gas reservoirs [33–35]. The cushion gas remains in the reservoir as a precautionary measure to maintain an operating pressure, limit the risks of induced seismic activity, and minimize hydrogen losses and groundwater intrusion.

It seems clear that part of the stored H_2 is used as a cushion gas in storage in saline structures, since it avoids harmful effects of mixing, dilution, and reactivity with other gases [36,37]. In the case of underground storage in depleted hydrocarbon reservoirs and aquifers, other authors suggest the possibility of using CH_4 as a cushion gas because of its residual presence, and CO_2 and N_2 because of their higher wettability, density, and viscosity than H_2, to facilitate both their separation during injection/extraction cycles and, if necessary, the displacement of water [29,31].

The use of mines in Mesozoic and Tertiary salt deposits [38], such as those located in northeastern Spain, presents a flexible and efficient option for green hydrogen storage. The use of wells, galleries, chimneys, and ramps would drastically reduce the costs and execution times of underground storage. The mine infrastructure would allow the development of lining, ventilation, and geotechnical control of the storage cavern, increasing its tightness and safety conditions.

5. Conclusions

The saline diapirs constitute safe hydrogen gas storages, allowing injection-extraction cycles in the short and long term. The creep phenomenon determines the cavern generation process and well stability in hydrogen storage and production processes.

The parameters that have the greatest influence are the tensional state and temperature, and it is necessary that the drilling mud of the well exerts a hydrostatic pressure equal to the horizontal tension, and that an aqueous mud saturated in salt is considered in order to avoid the dissolution of the walls of the well. The casing design must be devised according to the rock stresses and cementing of the well using cement having high salt concentrations. Control or monitoring of the design parameters during salt rock leaching will ensure the correct shape and dimensions.

The shape of the cavity affects the spatial distribution of stresses, the convergence of the salt rock, and the volume loss of the cavern. The geometry of the capsule-shaped cavern, of cylindrical design with a hemispherical shape at the top and bottom, ensures a low stress state and lower convergence. The geomechanical safety of the cavern is conditioned by the gas pressure inside the cavern remaining within a given range. The rate of injection and extraction of hydrogen from the cavern is therefore limited by the maximum and minimum pressure, by the maximum pressure change per unit of time that allows its stability, and by the maximum flow velocity inside the production pipe, which depends on its diameter. The operation of the caverns must be carried out under safe conditions, so as to minimize the risks to the environment and people.

The Poza de la Sal salt dome meets the geological, technical-economic, and environmental criteria for renewable hydrogen storage. During the filling stage, the injection ratio is higher than the extraction ratio due to the variation in hydrogen density related to the pressure in the cavity, which increases during the filling of the cavern. It is necessary to carry out simulation studies to control the variables that may affect the injection ratio, in order to adjust the injection-extraction flow rate in each case.

The storage capacity is calculated based on thermodynamic considerations according to specific storage data. Taking into account the surplus of wind energy production in the Autonomous Community of Castilla y León during the months of October to June 2020, production of 503 GWh is available for the production of storable hydrogen. During this period, a wind energy surplus of 23 GWh was obtained in the Páramo de Poza WP.

The construction of two caverns, having a capacity of 396 GWh each, is proposed as an option, which would make it possible to store all the surplus wind energy in Castilla y León; one may be used to store surplus energy from the wind park, and the other for hydrogen production. The sale to the chemical industry of the brine obtained in the leaching phase can result in a benefit to the project.

Author Contributions: Conceptualization, L.M.V.-F., C.G.-O., L.F.M.-M., A.H.-B. and S.E.-D.; Supervision, L.M.V.-F. and C.G.-O.; Validation, L.M.V.-F., C.G.-O., L.F.M.-M., A.H.-B., S.E.-D. and R.R.-P.; Writing—original draft, L.M.V.-F. and C.G.-O.; Writing—review & editing, L.M.V.-F., C.G.-O., L.F.M.-M., A.H.-B., S.E.-D. and R.R.-P. All authors have read and agreed to the published version of the manuscript.

Funding: This research was funded by the Oil and Gas Engineering Master's degree (mip) of the Universidad Politécnica de Madrid (UPM), which is taught at the Escuela Técnica Superior de Ingenieros de Minas y Energía (ETSIME).

Institutional Review Board Statement: Not applicable.

Informed Consent Statement: Not applicable.

Data Availability Statement: Not applicable.

Conflicts of Interest: The authors declare no conflict of interest.

Abbreviation

Nomenclature (unit)	
C	Working gas energy (kWh)
D	Cavern diameter (m)
g	Gravity acceleration (m/s^2)
H	Cavern height (m)
M	Molecular mass of hydrogen (kg/mol)
m_{base}	Base gas mass (kg)
m_{work}	Working gas mass (kg)
m_t	Total gas mass [m_{base}+m_{work}] (kg)
P	Lithostatic or overload pressure (Pa)
$P_{min/max}$	Operating pressure min/max (Pa)
R_0	Gas constant (J/K·mol)
R	Cavern Radius (m)
T_a	Average cavity temperature (°C)
T_{sup}	Ground surface temperature (°C)
V	Cavern volume (m^3)
z	Cavern base depth (m)
$Z_{1/2}$	Compressibility factor for P_{max}/P_{min}
Greek symbols (unit)	
∇T	Geothermal gradient (K/m)
ρ	Rock salt density (kg/m^3)
$\rho_{min/max}$	Gas density min/max (kg/m^3)
$\rho_{H2,min/max}$	Hydrogen density min/max (kg/m^3)
Abbreviations (unit)	
NC	Normal conditions (1 atm, 0 °C)
ECE	Energy consumed in electrolysis (GWh)
WES	Wind energy surplus (GWh)
LHV	Lower heating value of H_2 (kWh/kg)
WP	Wind park (MW)

References

1. Kupecki, J.; Skrzypkiewicz, M.; Błesznowski, M. Current advancements in hydrogen technology and pathways to meet decarbonisation. Towards hydrogen societies: Expert group meeting. In Proceedings of the 24th Session of the Conference of the Parties to the United Nations Framework, Convention on Climate Change (UNFCCC)—COP24, Lubelskie, Poland, 12 December 2018.
2. MITERD. *Hoja de Ruta del Hidrógeno: Una Apuesta por el Hidrógeno Renovable*; Ministerio para la Transición Ecológica y el Reto Demográfico: Madrid, Spain, 2020.
3. Ray, I.; Chakraborty, T.; Roy, D.; Datta, A.; Mandal, B. Production, storage and properties of hydrogen as internal combustion engine fuel: A critical review. *Nat. Gas* **2013**, *240*, 48.
4. Abe, I. Physical and chemical properties of hydrogen. In *Energy Carriers and Conversion Systems*; EOLSS Publications: Paris, France, 2009; Volume I. Available online: https://www.eolss.net/ebooklib/sc_cart.aspx?File=E3-13-01-01 (accessed on 21 April 2022).
5. Heinemann, N.; Alcalde, J.; Miocic, J.M.; Hangx, S.J.T.; Kallmeyer, J.; Ostertag-Henning, C.; Hassanpouryouzband, A.; Thaysen, E.M.; Strobel, G.J.; Schmidt-Hattenberger, C.; et al. Enabling large-scale hydrogen storage in porous media-the scientific challenges. *Energy Environ. Sci.* **2021**, *14*, 853–864. [CrossRef]
6. Las Energías Renovables en el Sistema Eléctrico Español 2020. Red Eléctrica de España. Available online: https://www.ree.es/sites/default/files/publication/2021/06/downloadable/informe_renovables_2020_0.pdf (accessed on 18 April 2022).
7. Ozarslan, A. Large-scale hydrogen energy storage in salt caverns. *Int. J. Hydrogen Energy* **2012**, 14265–14277. [CrossRef]
8. Steven, J.D.; Nathan, S.L.; Matthew, S.; Aggarwal, S.; Arent, D.; Azevedo, I.L.; Benson, S.M.; Bradley, T.; Brouwer, J.; Caldeira, K.; et al. Net-zero emissions energy systems. *Science* **2018**, *360*, 114–161. [CrossRef]
9. Schiebahn, S.; Grube, T.; Robinius, M.; Tietze, V.; Kumar, B.; Stolten, D. Power to gas: Technological overview, systems analysis and economic assessment for a case study in Germany. *Int. J. Hydrogen Energy* **2015**, *40*, 4285–4294. [CrossRef]
10. Bertuccioli, L.; Chan, A.; Hart, D.; Lehner, F.; Madden, B.; Standen, E. Study on Development of Water Electrolysis in the EU. Final Report. July 2014. Available online: https://www.fch.europa.eu/sites/default/files/study%20electrolyser_0.pdf (accessed on 29 April 2022).
11. Kruck, O.; Crotogino, F.; Prelicz, R.; Rudolph, T. Overview on All Known Underground Storage Technologies for Hydrogen. HyUnder. Grant Agreement 303417 Deliverable, August 2013; p. 93. Available online: http://hyunder.eu/wp-content/uploads/2016/01/D3.1_Overview-of-all-known-underground-storage-technologies.pdf (accessed on 12 May 2022).

12. Caglayan, D.G.; Weber, N.; Heinrichs, H.U.; Linßen, J.; Robinius, M.; Kukla, P.A.; Stolten, D. Technical potential of salt caverns for hydrogen storage in Europe. *Int. J. Hydrogen Energy* **2020**, *45*, 6793–6805. [CrossRef]
13. Schulze, O.; Popp, T.; Kern, H. Development of damage and permeability in deforming rock salt. *Eng. Geol.* **2001**, *61*, 163–180. [CrossRef]
14. Ruiz, C.; Martinez, R.; Recreo, F.; Prado, P.; Campos, R.; Pelayo, M.; Losa, A.D.L.; Hurtado, A.; Lomba, L.; Perez del Villar, L.; et al. Geological Storage of CO2. Site Selection Criteria. Madrid 2006. Ciemat-1085. p. 108. Available online: https://inis.iaea.org/collection/NCLCollectionStore/_Public/38/030/38030356.pdf?r=1 (accessed on 19 April 2022).
15. Robles, S.; Aranburu, A.; Apraiz, A. La Cuenca Vasco-Cantábrica: Génesis y evolución tectonosedimentaria. *Enseñ. Cienc. Tierra* **2014**, *22*, 99–114.
16. Pedreira, D. Estructura de la Zona de Transición de los Pirineos y la Cordillera Cantábrica. Ph.D. Thesis, Universidad de Oviedo, Oviedo, Spain, 2004; pp. 1–343.
17. Khaledi, K.; Mahmoudi, E.; Datcheva, M.; Tom Schanz, T. Stability and serviceability of underground energy storage caverns in rock salt subjected to mechanical cyclic loading. *Int. J. Rock. Mech. Min.* **2016**, *86*, 115–131. [CrossRef]
18. Howard, B.J.S.; Veldhuis, I.; Neil Richardson, R. Underground hydrogen storage in the UK. *Geol. Soc. Lond. Spec. Publ.* **2009**, *313*, 217–226. [CrossRef]
19. Korzeniowski, W.; Poborska-Młynarska, K.; Skrzypkowski, K.; Zagórski, K.; Chromik, M. Cutting Niches in Rock Salt by Means of a High-Pressure Water Jet in Order to Accelerate the Leaching of Storage Caverns for Hydrogen or Hydrocarbons. *Energies* **2020**, *13*, 1911. [CrossRef]
20. Barker, J.W.; Feland, K.W.; Tsao, Y.-H. Drilling Long Salt Sections Along the U.S. Gulf Coast. *SPE Drill. Completion* **1994**, *9*, 185–188. [CrossRef]
21. Wang, H.; Samuel, R. Geomechanical Modeling of Wellbore Stability in Salt Formations. *Soc. Pet. Eng.* **2014**, *31*, 261–272. [CrossRef]
22. Cyran, K.; Kowalski, M. Shape Modelling and Volumen Optimisation of Salt Caverns for Energy Storage. *Appl. Sci.* **2021**, *11*, 423. [CrossRef]
23. Papadias, D.D.; Ahluwalia, R.K. Bulk storage of hydrogen. *Int. J. Hydrogen Energy* **2021**, *46*, 34527–34541. [CrossRef]
24. Barron, T.F. Regulatory, technical pressures prompt more US salt-cavern gas storage. *Oil Gas J.* **1994**, *92*, 55–67. [CrossRef]
25. Portarapillo, M.; Di Benedetto, A. Risk Assessment of the Large-Scale Hydrogen Storage in Salt Caverns. *Energies* **2021**, *14*, 2856. [CrossRef]
26. Albrecht, U.; Bünger, U.; Michalski, J.; Raksha, T.; Wurster, R.; Zerhusen, J. International Hydrogen Strategies. A Study Commissioned by and in Cooperation with the World Energy Council Germany 2020. Final Report. Available online: https://www.researchgate.net/publication/345163207 (accessed on 12 April 2022).
27. Bell, I.H.; Wronski, J.; Quoilin, S.; Lemort, V. Pure and pseudo-pure fluid thermophysical property evaluation and the open-source thermophysical property library coolprop. *Ind. Eng. Chem. Res.* **2014**, *53*, 2498–2508. [CrossRef]
28. Londe, L. Hydrogen Caverns Are a Proven, Inexpensive and Reliable Technology. 2018. Available online: https://medium.com/@ch2ange (accessed on 9 May 2022).
29. Sainz-Garcia, A.; Abarca, E.; Rubi, V.; Grandia, F. Assessment of feasible strategies for seasonal underground hydrogen storage in a saline aquifer. *Int. J. Hydrogen Energy* **2017**, *42*, 16657–16666. [CrossRef]
30. Cihlar, J.; Mavins, D.; Van der Leun, K. *Picturing the Value of Underground Gas Storage to the European Hydrogen System*; Guidehouse: Chicago, IL, USA, 2021; p. 52.
31. Panfilov, M. Underground and pipeline hydrogen storage. In *Compendium of Hydrogen*; Gupta, R.B., Ed.; Elsevier: Amsterdam, The Netherlands, 2016; p. 92.
32. He, T.; Rong, Z.; Zheng, J.; Ju, Y.; Linga, P. LNG cold energy utilization: Prospects and challenges. *Energy* **2019**, *170*, 557–568. [CrossRef]
33. Bai, M.; Song, K.; Sun, Y.; He, M.; Li, Y.; Sun, J. An overview of hydrogen underground storage technology and prospects in China. *J. Pet. Sci. Eng.* **2014**, *124*, 132–136. [CrossRef]
34. Lord, A.S.; Kobos, P.H.; Borns, D.J. Geologic storage of hydrogen: Scaling up to meet city transportation demands. *Int. J. Hydrogen Energy* **2014**, *39*, 15570–15582. [CrossRef]
35. Wallace, R.L.; Cai, Z.; Zhang, H.; Zhang, K.; Guo, C. Utility-scale subsurface hydrogen storage: UK perspectives and technology. *Int. J. Hydrogen Energy* **2021**, *46*, 25137–25159. [CrossRef]
36. Heinemann, N.; Scafidi, J.; Pickup, G.; Thaysen, E.M.; Hassanpouryouzb, A.; Wilkinson, M.; Satterley, A.K.; Booth, M.G.; Edlmann, K.; Haszeldine, R.S. Hydrogen storage in saline aquifers: The role of cushion gas for injection and production. *Int. J. Hydrogen Energy* **2021**, *46*, 39284–39296. [CrossRef]
37. Hemme, C.; Van Berk, W. Hydrogeochemical Modeling to Identify Potential Risks of Underground Hydrogen Storage in Depleted Gas Fields. *Appl. Sci.* **2018**, *8*, 2282. [CrossRef]
38. Crotogino, F.; Donadei, S.; Bünger, U.; Landinger, H. Large-scale hydrogen underground storage for securing future energy supplies. In Proceedings of the 18th World Hydrogen Energy Conference 2010—WHEC 2010, Zürich, Switzerland, 16–21 May 2010; pp. 37–45.